


Mediator subunit MDT-15 promotes expression of propionic acid breakdown genes to prevent embryonic lethality in *Caenorhabditis elegans*

Grace Ying Shyen Goh,^{1,2,3,4} Arshia Beigi,^{2,3,5} Junran Yan,^{1,2,3} Kelsie R.S. Doering,^{2,3,6} Stefan Taubert ^{1,2,3,6,*}

¹Graduate Program in Cell & Developmental Biology, The University of British Columbia, 950 W 28th Ave, Vancouver, BC V5Z 4H4, Canada

²Centre for Molecular Medicine and Therapeutics, The University of British Columbia, 950 W 28th Ave, Vancouver, BC V5Z 4H4, Canada

³British Columbia Children's Hospital Research Institute, 950 W 28th Ave, Vancouver, BC V5Z 4H4, Canada

⁴Present address: Semios Biotechnologies, 3430 Brighton Ave #204A, Burnaby, BC V5A 3H4, Canada

⁵Present address: Department of Medicine, University of British Columbia, 2775 Laurel Street, Vancouver, BC V5Z 1M9, Canada

⁶Department of Medical Genetics, The University of British Columbia, 950 W 28th Ave, Vancouver, BC V5Z 4H4, Canada

*Corresponding author: Centre for Molecular Medicine and Therapeutics, Room 2024, 950 W 28th Avenue, Vancouver, BC V5Z 4H4, Canada. Email: taubert@cmmt.ubc.ca

Abstract

The micronutrient vitamin B12 is an essential cofactor for two enzymes: methionine synthase, which plays a key role in the one-carbon cycle; and methylmalonyl-CoA mutase, an enzyme in a pathway that breaks down branched-chain amino acids and odd-chain fatty acids. A second, vitamin B12-independent pathway that degrades propionic acid was recently described in *Caenorhabditis elegans*, the propionate shunt pathway. Activation of five shunt pathway genes in response to low vitamin B12 availability or high propionic acid levels is accomplished by a transcriptional regulatory mechanism involving two nuclear hormone receptors, NHR-10 and NHR-68. Here, we report that the *C. elegans* Mediator subunit *mdt-15* is also essential for the activation of the propionate shunt pathway genes, likely by acting as a transcriptional coregulator for NHR-10. *C. elegans mdt-15* mutants fed with a low vitamin B12 diet have transcriptomes resembling those of wild-type worms fed with a high vitamin B12 diet, with low expression of the shunt genes. Phenotypically, the embryonic lethality of *mdt-15* mutants is specifically rescued by diets high in vitamin B12, but not by dietary polyunsaturated fatty acids, which rescue many other phenotypes of the *mdt-15* mutants. Finally, NHR-10 binds to MDT-15 in yeast two-hybrid assays, and the transcriptomes of *nhr-10* mutants share overlap with those of *mdt-15* mutants. Our data show that MDT-15 is a key coregulator for an NHR regulating propionic acid detoxification, adding to roles played by NHR:MDT-15 partnerships in metabolic regulation and pinpointing vitamin B12 availability as a requirement for *mdt-15* dependent embryonic development.

Keywords: propionic acid, vitamin B12, Mediator complex, MED15, gene expression

Introduction

Animals adjust their metabolism based on their nutritional environment, which allows them to optimize the use of available resources and adjust to or compensate for absent or limiting nutrients. Such metabolic adjustments occur through various mechanisms, including alteration in the expression of metabolic and other genes via transcriptional modulation. Regulation can involve direct sensing of nutritional components or metabolites by transcription factors such as nuclear hormone receptors (NHRs) and indirect sensing via upstream regulators such as G protein-coupled receptors or other sensors (Boukouris et al. 2016; Husted et al. 2017; Schneider-Poetsch and Yoshida 2018; Suganuma and Workman 2018).

Vitamins are a group of essential micronutrients required in many developmental and physiological functions. All animals require vitamin B12, which is vital for DNA synthesis, and fatty acid and amino acid metabolism (Deodato et al. 2017; Froese et al. 2019). Vitamin B12 is an essential cofactor for methylmalonyl-CoA mutase (MUT),

an enzyme in the canonical and evolutionarily conserved propionic acid breakdown pathway (Bito and Watanabe 2016; Deodato et al. 2017; Froese et al. 2019). The loss of activity in this pathway due to mutations in the MUT gene or in the genes for propionyl-CoA-carboxylase (PCCA/B) causes the inborn errors of metabolism methylmalonic acidemia and propionic acidemia, respectively (Deodato et al. 2017). Abnormal metabolism in these genetic diseases severely affects development and neurological functions and can cause lethality in newborns.

Recent work in *Caenorhabditis elegans* has revealed the existence of a parallel, vitamin B12-independent propionic acid breakdown pathway, termed the propionic acid breakdown shunt ('the shunt') (Watson et al. 2016). The shunt is composed of enzymes that are conserved in humans (*acd1-1/ACACB*, *ech-6/ECHS1*, *hach-1/HIBCH*, *hpdh-1/ADHFE1*, and *alh-8/ALDH6A1*) (Watson et al. 2016). However, as intermediate metabolites of the shunt are toxic, shunt gene expression is repressed except when the pathway is absolutely required. In *C. elegans*, conditions of low dietary vitamin B12 or high dietary propionic acid result in

Received: December 16, 2022. Accepted: April 17, 2023

© The Author(s) 2023. Published by Oxford University Press on behalf of The Genetics Society of America.

This is an Open Access article distributed under the terms of the Creative Commons Attribution License (<https://creativecommons.org/licenses/by/4.0/>), which permits unrestricted reuse, distribution, and reproduction in any medium, provided the original work is properly cited.

increased shunt gene expression (MacNeil et al. 2013; Watson et al. 2013, 2014, 2016).

The tight regulation of shunt genes in *C. elegans* is achieved by combinatorial activity of NHR-10 and NHR-68 (Bulcha et al. 2019). Both NHRs are required to induce shunt gene expression and for organismal survival on diets with high propionic acid levels. Interestingly, NHR-10 itself activates *nhr-68*, yet, *nhr-68* expression alone is insufficient to induce the propionate shunt genes; rather, *nhr-10* and *nhr-68* are both required for this activation, and hence, form a self-reinforcing regulatory circuit that only results in gene activation when elevated propionic acid levels persist in the media for several hours (Bulcha et al. 2019).

Like all transcription factors, NHRs do not act in isolation but require coregulators to control gene expression. In *C. elegans*, the Mediator subunit MDT-15 is a coregulator for many NHRs that regulate nutritional and stress adaptive responses (Grants et al. 2015; Hartman et al. 2021). Accordingly, *mdt-15* mutation or depletion results in many developmental and physiological phenotypes, many of which can be rescued by supplementation with unsaturated fatty acids (Taubert et al. 2006; Yang et al. 2006; Hou et al. 2014; Lee et al. 2015, 2019). However, some phenotypes of the *mdt-15* mutant cannot be rescued by unsaturated fatty acids, suggesting that other dietary processes and metabolic regulatory pathways may be linked to *mdt-15* (Goh et al. 2014, 2018).

Here, we show that transcriptomic changes caused by *mdt-15* loss resemble those of worms grown on a low vitamin B12 diet, with shunt genes downregulated in both conditions. Supplementation with vitamin B12-rich diets, but not with unsaturated fatty acids, rescued the embryonic lethality of *mdt-15* mutants. NHR-10, which controls shunt gene expression, physically interacts with MDT-15, and loss of either regulator produces similar transcriptomic perturbations. Our data suggest a model wherein *C. elegans* MDT-15 acts as a coregulator for NHR-10, with the two factors inducing shunt genes on demand to ensure propionic acid detoxification and prevent adverse organismal phenotypes.

Materials and methods

C. elegans growth conditions

We cultured *C. elegans* strains using standard techniques on nematode growth media (NGM) plates, as described (Brenner 1974). NGM plates were supplemented at the indicated concentrations with methyl-cobalamin (Me-Cbl; Sigma M9756), adenosyl-cobalamin (Ado-Cbl; Sigma C0884), propionic acid (Sigma 402907), tert-butyl-hydroperoxide (tBOOH) (Sigma 458139), and polyunsaturated fatty acids (PUFAs; mix of fatty acid sodium salts: 150 μ M C18:2, S-1127; 150 μ M C20:5, S-1144, Nu-Chek Prep). *Escherichia coli* OP50 and *Comamonas aquatica* DA1877 were used as food sources, as indicated. For food source switching experiments, P0 animals were grown on either *E. coli* OP50 or *C. aquatica* DA1877 food; from these P0 cultures, F1 embryos were then harvested by sodium hypochlorite bleaching and placed on the same or other food source until larval development was complete (~48 hours after embryo collection). *fat-6* RNAi experiments were performed with *E. coli* HT115 on NGM plates supplemented with 100 μ g/ml carbenicillin (BioBasic CDJ469), 1 mm IPTG (Santa Cruz, sc-202185B), and 12.5 μ g/ml tetracycline (BioBasic TB0504). RNAi clones were from the Ahringer (Source BioScience) and were sequenced prior to use. All experiments were carried out at 20°C.

C. elegans strains

Worm strains used in this study were N2 wild type (WT) and XA7702 *mdt-15(tm2182)* (Taubert et al. 2008); the mutant was

backcrossed into our lab N2 strain prior to study. For synchronized worm growths, we isolated embryos by standard sodium hypochlorite treatment. Isolated embryos were allowed to hatch overnight on unseeded NGM plates until the population reached a synchronized state of halted development at L1 stage via short-term fasting (16–24 hours). Synchronized L1 stage larvae were then transferred to seeded plates and grown to the desired stage.

Embryo viability assays

WT N2 and XA7702 *mdt-15(tm2182)* worms were grown to young adults on NGM plates seeded with *E. coli* OP50 or *C. aquatica* DA1877. Then, 10 worms were transferred onto plates seeded with *E. coli* OP50 or *C. aquatica* DA1877 and left at 20°C for 24 hours. Adults were then removed, and progeny were allowed to hatch for 48 hours. Eggs that had not hatched thereafter were classified as nonviable.

Oxidative stress sensitivity assays

To assess oxidative stress sensitivity, synchronized N2 and *mdt-15(tm2182)* L1 stage worms were allowed to grow on NGM plates containing 300 μ M PUFAs and/or 5 nM vitamin B12 until they reached the mid-L4 stage. Then, they were transferred to plates also containing 2 or 4 mM tBOOH, which were seeded with heat-inactivated *E. coli* OP50. After 24 hours, the number of dead or alive worms was counted. In parallel, to ascertain PUFA effectiveness, we also scored whether PUFA supplementation was able to rescue viability of N2 on RNAi plates seeded with HT115 bacteria containing control empty vector (EV) of *fat-6* RNAi clones.

RNA isolation and RT-qPCR analysis

Synchronized L1 worms were allowed to grow on *E. coli* OP50 plates for 48 hours to L4 stage and rapidly harvested. RNA isolation was performed as previously described (Doering et al. 2022). Briefly, 2 μ g total RNA was used to generate cDNA with Superscript II reverse transcriptase (Invitrogen 18064-014), random primers (Invitrogen 48190-011), dNTPs (Fermentas R0186), and RNaseOUT (Invitrogen 10777-019). Quantitative PCR was performed in 10 μ l reactions using Fast SYBR Master Mix (Life Technologies 4385612), 1:10 diluted cDNA, and 5 μ M primer, and analyzed with an Applied Biosystems StepOnePlus machine. We analyzed the data with the $\Delta\Delta$ Ct method. For each sample, we calculated normalization factors by averaging the (sample expression)/(average reference expression) ratios of three normalization genes, *act-1*, *tba-1*, and *ubc-2*. The reference sample was wild type (WT) grown on *E. coli* OP50. We used one-way or two-way ANOVA to calculate statistical significance of gene expression changes and corrected for multiple comparisons using the Tukey method. Primers were tested on serial cDNA dilutions and analyzed for PCR efficiency prior to use. All data originate from three or more independent biological repeats, and each PCR reaction was conducted in technical duplicate. Sequences of RT-qPCR primers are listed in Table 1.

Microarray analysis

Microarray gene expression profiling of *mdt-15(tm2182)* mutants was performed at the University of California San Francisco SABRE Functional Genomics Facility exactly as previously described (Grants et al. 2016), using the same growth conditions, and RNA extraction, processing, hybridization, and analysis methods. Microarray data of *mdt-15(tm2182)* mutants and corresponding WT are deposited in Gene Expression Omnibus (GEO) under a new accession number (GSE220955), with the WT control exactly the same as previously published [GEO Series GSE68520 (Grants et al. 2016)]. Microarray data were processed using limma (Ritchie et al. 2015) exactly as described (Grants et al. 2016). To

Table 1. Sequences of primers used in this study.

Gene	Acc. no.	Fwd primer	Rev primer
<i>act-1</i>	T04C12.6	gctggacgtgatcttactgattacc	gtagcagagcttctcttgatgtc
<i>ubc-2</i>	M7.1	agggaggtgtcttctctctcac	cggatttggatcacagagcagc
<i>tba-1</i>	F26E4.8	gtacctccactgatctctgctgacaag	ctctgtacaagaggcaaacagccatg
<i>acdh-1</i>	C55B7.4	acagagagaacagttcggtc	gtgatgcaaacagtttcgcc
<i>hphd-1</i>	Y38F1A.6	tctttgtgatcggctgagag	gatccgcagacttggagag
<i>hach-1</i>	F09F7.4	attgtgatggaggaggttg	tctgggaagatccaagtgc
<i>ech-6</i>	T05G5.6	ggttctcggggaagctgtg	ctcttctcggcaaaagcgg

maximize comparability of the microarray to RNA-seq datasets, probe identifiers were converted to gene symbols using the ID conversion module of easyGSEA in the eVITTA toolbox (Cheng et al. 2021), and only the highest expressing probe (based on aveA average expression) was kept for each unique gene symbol. Using this approach, we identified 1,616 unique differentially expressed genes (DEGs) with $\text{Adj.}P < 0.05$ in *mdt-15(tm2182)* mutants, including 563 downregulated ($\log_{2}FC < 0$) and 1,053 upregulated ($\log_{2}FC > 0$) genes (Supplementary Tables 1 and 2).

Reanalysis of published microarray data

To maximize comparability with our microarray samples, we reanalyzed published two-channel microarray data of *mdt-15(RNAi)* worms (Taubert et al. 2008). Raw data were extracted from GEO under the accession number GSE9720 and reanalyzed with limma. Adaptive background correction was performed with the method “normexp” with offset 50, and subsequently normalizeWithinArrays using default method (print tip loess). The command modelMatrix with set reference level “control RNAi” was used to make the sign of M consistent across repeats regardless of dye swapping. Differentially expressed genes were computed using lmFit, eBayes, and topTable with the default parameters, and probe identifiers were converted to unique gene symbols as above. We identified 2,451 DEGs with $P < 0.05$, including 1,298 downregulated and 1,153 upregulated genes (Supplementary Tables 1 and 3).

We also reanalyzed the published single-channel microarray of *Comamonas* DA1877 vs *E. coli* HT115 treatment (MacNeil et al. 2013), for which normalized count data are available in GEO (accession number: GSE43959). We performed data extraction and differential expression (DE) analysis using easyGEO in the eVITTA toolbox (Cheng et al. 2021), using default parameters (limma with quantile normalization and linear model fitting with ls). Probe identifiers were converted to unique gene symbols as above. We identified 6,541 DEGs with $P < 0.05$, including 2,979 downregulated and 3,562 upregulated genes (Supplementary Tables 1 and 4).

Reanalysis of published RNA-seq data

To maximize comparability with our microarray samples, we reanalyzed published RNA-sequencing data of Vitamin B12-treated WT worms, and of *nhr-10* and *nhr-68* mutants (Bulcha et al. 2019). Relevant Sequence Read Archive (SRA) accession numbers and metadata were obtained from SRA run selector under the GEO accession number GSE123507. For each SRA accession number, raw reads were downloaded from SRA using prefetch, and FASTQ files were extracted using fastq-dump. Because the study was done on BGI-seq-500 platform, we compiled a list of adaptor sequences using the overrepresented sequences from FastQC. Following this, the reads were trimmed using Trimmomatic version 0.36 (Bolger et al. 2014) with parameters LEADING:3 TRAILING:3 SLIDINGWINDOW:4:15 MINLEN:36. Next, trimmed reads were aligned to the NCBI reference genome WBcel235 WS277 (https://www.ncbi.nlm.nih.gov/assembly/GCF_000002985.6/) using Salmon

version 0.9.1 (Patro et al. 2017) with parameters `-l A -gcBias -validateMappings`. Then, transcript-level read counts were imported into R and summed into gene-level read counts using tximport (Soneson et al. 2016). Genes not expressed at a level greater than one count per million reads in at least two of the samples were excluded from further analysis. The gene-level read counts were normalized using the trimmed mean of M-values in edgeR (Robinson et al. 2010) to adjust samples for differences in library size. Differential expression analysis was performed using the quasi-likelihood F-test with the generalized linear model approach in edgeR (Robinson et al. 2010). The number of upregulated and downregulated DEGs is found in Supplementary Table 1, and all DEGs are listed in Supplementary Tables 5–7.

Comparison and visualization of transcriptome data

As quality controls, we compared genes deregulated in *mdt-15(tm2182)* mutants to genes deregulated in *mdt-15(RNAi)* worms (GSE9720), revealing a substantial correlation between the two datasets (Supplementary Fig. 1a), as expected. The scatter plot was generated using plotly, and Pearson correlation coefficient was computed using the cor.test function.

To visualize the downregulation of shunt genes in different datasets, we generated volcano plots using limma function plotWithHighlights. We separated DEGs (defined as the genes with $\text{Adj.}P$ or $P < 0.05$) above the line, and shunt genes were marked using additional text labels.

To compare our microarray data to previously published data, we generated Venn diagrams using the R package eulerr (Larsson and Gustafsson 2018). Hypergeometric P -value was calculated using the phyper function, where q = size of overlap 1, m = number of genes in gene list 1, n = platform size m , and k = number of genes in gene list 2. For each pairwise comparison, platform size was calculated as the total number of genes that are detected in DE analysis in either sample.

For overrepresentation analysis (ORA) of gene list overlaps, we analyzed lists of downregulated genes ($\text{Adj.}P$ or $P < 0.05$, and $\log_{2}FC < 0$) using the ORA module of easyGSEA in the eVITTA toolbox (Cheng et al. 2021). The following gene set databases were selected for ORA analysis: Kyoto Encyclopedia of Genes and Genomes (KEGG), Reactome Pathway (RA), WikiPathways (WP), WormCat Category 2 (C2), WormCat Category 3 (C3), and Gene Ontology: Biological Processes (BP). Top 10 significantly enriched gene sets ($P < 0.005$ and $\text{Adj.}P < 0.25$) were visualized using the bar plot module. The shunt genes in each gene set are annotated in the plots.

Results

Transcriptomes of *mdt-15* mutants partially resemble those of worms grown on *C. aquatica*

We and others found that *mdt-15(RNAi)* and *mdt-15(tm2182)* hypomorph mutants display phenotypes such as embryonic lethality,

delayed larval development, reduced body size, reduced fecundity, fat storage defects, axon migration defects, stress sensitivity, impaired locomotion, and short life span (Taubert et al. 2006, 2008; Yang et al. 2006; Arda et al. 2010; Steimel et al. 2013; Goh et al. 2014, 2018; Pukkila-Worley et al. 2014; Lee et al. 2015, 2019; Vozdek et al. 2018; Peterson et al. 2019; Shomer et al. 2019; Doering et al. 2022). *mdt-15* inactivation compromises fatty acid desaturation, and PUFA supplementation of worms with reduced *mdt-15* function improves many of the above phenotypes, robustly rescuing larval development, body size, locomotion, fecundity, and life span (Taubert et al. 2006; Yang et al. 2006; Lee et al. 2015, 2019). In contrast, the oxidative stress sensitivity and altered zinc storage of *mdt-15* mutants are not rescued by PUFA supplementation (Goh et al. 2014; Shomer et al. 2019). Similarly, the embryonic lethality of *mdt-15(tm2182)* hypomorph mutants is unaffected by PUFA supplementation (see below), suggesting that other, unknown dysregulated processes must underlie this phenotype.

To identify *mdt-15* dependent processes that may promote PUFA-independent embryonic development, we compared transcriptome profiles of *mdt-15(RNAi)* and *mdt-15(tm2182)* hypomorph mutants to other transcriptomes. We found that the transcriptomes of WT worms fed with the bacterial food source *C. aquatica* DA1877 (MacNeil et al. 2013) shared a statistically significant overlap with genes dependent on *mdt-15* (Fig. 1a). Vitamin B12 (aka cobalamin) is a key molecule that drives *C. aquatica*-induced developmental acceleration and it is virtually undetectable in *E. coli* OP50 (Watson et al. 2014). Accordingly, the transcriptomes of worms grown on vitamin B12 supplemented OP50 (Bulcha et al. 2019) also shared a statistically significant overlap with genes dependent on *mdt-15* (Fig. 1b). Thus, the loss of *mdt-15* results in transcriptomes that partially resemble those of worms fed with vitamin B12-rich diets.

A diet of *C. aquatica* rescues the embryonic lethality of *mdt-15(tm2182)* mutants

To determine if a diet of *C. aquatica* DA1877 might influence the phenotypes of *mdt-15(tm2182)* mutants, we compared *mdt-15(tm2182)* mutants fed with *C. aquatica* DA1877 or *E. coli* OP50. We observed a substantial increase in the number of viable *mdt-15(tm2182)* mutant offspring when provided with *C. aquatica* DA1877 (Fig. 2a). To determine whether maternal or offspring food source caused the phenotypic rescue, we grew *mdt-15(tm2182)* mutants to adulthood on either *E. coli* OP50 or *C. aquatica* DA1877, switched them to the identical or reciprocal food sources, and then quantified the number of surviving offspring. We found that adult *mdt-15(tm2182)* mutants raised on *E. coli* OP50 generated mostly arrested progeny even when switched to *C. aquatica* DA1877, whereas the progeny of worms raised on *C. aquatica* DA1877 mostly hatched successfully even when the adults were switched to an *E. coli* OP50 diet (Fig. 2b). Thus, maternal *C. aquatica* DA1877 is sufficient to rescue the embryonic lethality in *mdt-15(tm2182)* progeny.

Vitamin B12 rescues the embryonic lethality in *mdt-15(tm2182)* mutants

Vitamin B12 is the key component of *C. aquatica*-induced developmental acceleration (Watson et al. 2014). To determine whether vitamin B12 underlies the *C. aquatica*-induced rescue of the embryonic lethality of *mdt-15(tm2182)* mutants, we grew them on plates supplemented with 50 nM Me-Cbl, one of the active forms of vitamin B12 (Froese et al. 2019). Me-Cbl supplementation strongly rescued the embryonic lethality of *mdt-15(tm2182)*

mutants (Fig. 2c). Supplementation with 5 or 500 nM of Me-Cbl had a similar effect, and supplementation with 5, 50, or 500 nM Ado-Cbl, another active form of vitamin B12, also effectively rescued embryonic lethality at all concentrations (Fig. 2d). These data show that vitamin B12 levels are essential for normal embryonic viability of *mdt-15* mutants.

mdt-15(tm2182) mutants are sensitive to propionic acid

In *C. elegans*, vitamin B12 is required as a cofactor for two enzymes: the methionine synthase *metr-1*; and the MUT-type isomerase *mmcm-1* (Watson et al. 2016). We reasoned that methionine is unlikely to be in short supply in *C. elegans* strains feeding on *E. coli* as food source and thus did not study methionine metabolism. The other *C. elegans* enzyme that utilizes vitamin B12 as a cofactor is *mmcm-1*, which is required to clear propionic acid, a toxic intermediate in the catabolism of odd-chain fatty acids and branched-chain amino acids (Watson et al. 2016). To determine whether *mdt-15(tm2182)* mutants are sensitive to propionic acid, we placed L4 WT and *mdt-15* mutant worms grown with or without Me-Cbl on varying concentrations of propionic acid and monitored their survival after 24 hours. Almost 100% of WT worms survived in the presence of 20 mM propionic acid, whether or not supplemented with Me-Cbl; in contrast, <2.5% of *mdt-15(tm2182)* mutants survived in the presence of 20 mM propionic acid (Fig. 2e). At concentrations between 10 and 20 mM propionic acid, *mdt-15(tm2182)* mutants showed intermediate viability that was significantly rescued by the addition of Me-Cbl (Fig. 2e). Thus, the loss of *mdt-15* renders *C. elegans* sensitive to propionic acid, and this can be rescued by increasing the activity of vitamin B12 dependent propionic acid degradation pathway.

Unsaturated fatty acids do not rescue the embryonic lethality of *mdt-15* mutants

mdt-15 is required to express genes for unsaturated fatty acid synthesis (Taubert et al. 2006; Yang et al. 2006; Hou et al. 2014). To determine whether lack of unsaturated fatty acids contributes to the embryonic lethality phenotype of *mdt-15(tm2182)* mutants, we grew them on plates containing unsaturated fatty acids, vitamin B12, or a combination of both. Unlike vitamin B12, unsaturated fatty acids did not improve embryonic lethality (Fig. 3a). Fatty acid supplementation was effective in these experiments, as it rescued the reduced brood size of *fat-6(RNAi)* worms (Fig. 3b), as published (Yang et al. 2006).

Besides embryonic lethality, the oxidative stress sensitivity of *mdt-15(tm2182)* mutants is also not rescued by dietary supplementation with PUFAs (Goh et al. 2014). We therefore tested whether supplementation with PUFAs, vitamin B12, or a combination of both could rescue the sensitivity of *mdt-15(tm2182)* mutants to the pro-oxidant tBOOH. As before (Goh et al. 2014), PUFA supplementation had no effects. Similarly, Me-Cbl supplementation, either alone or in combination with PUFAs, failed to increase tBOOH resistance in *mdt-15(tm2182)* mutant worms (Fig. 3c), suggesting that this phenotype is not related to vitamin B12 dependent metabolism.

mdt-15 is required to express enzymes in the propionic acid shunt breakdown pathway

Propionic acid is degraded via two pathways in *C. elegans*: the “canonical”, vitamin B12 dependent pathway and the shunt pathway that is activated and critical when vitamin B12 is low or unavailable (Watson et al. 2016). Notably, four of five shunt pathway enzymes (*acdh-1*, *ech-6*, *hach-1*, and *hphd-1*), which are repressed

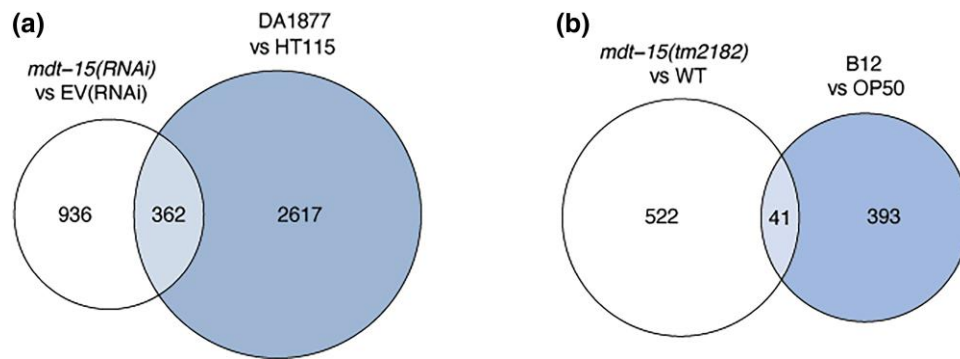


Fig. 1. Genes regulated by *mdt-15* overlap with genes regulated by vitamin B12-rich diets. a) The Venn diagram shows overlaps of genes downregulated in *mdt-15*(RNAi) worms and in worms grown on vitamin B12-rich *C. aquatica* DA1877 ($P < 0.05$ and $\log_{2}FC < 0$). Hypergeometric $P = 4.37e^{-28}$; platform size = 18,286. b) The Venn diagram shows overlaps of genes downregulated in *mdt-15*(*tm2182*) worms and in worms grown on an *E. coli* OP50 diet supplemented with vitamin B12 (Adj. P or $P < 0.05$ and $\log_{2}FC < 0$). Hypergeometric $P = 1.31e^{-10}$; platform size = 18,536. Lists of genes in each dataset are shown in [Supplementary Tables 2-5](#).

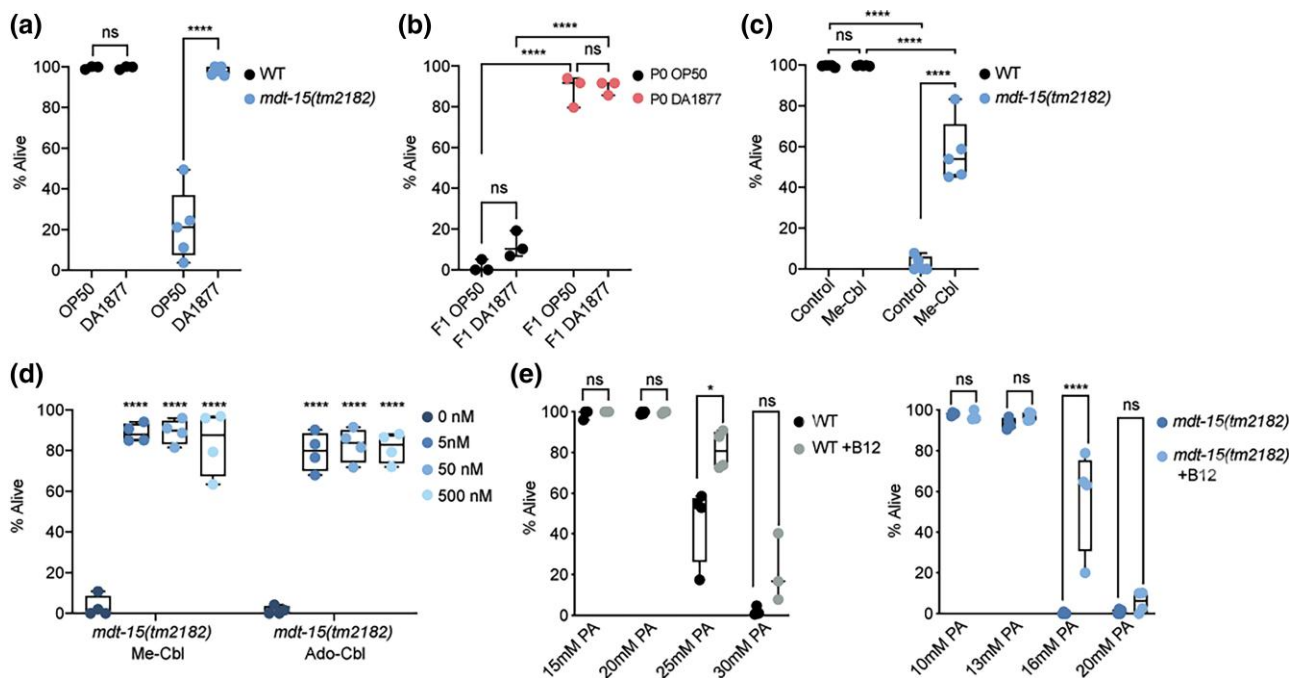


Fig. 2. Diets rich in vitamin B12 rescue the embryonic lethality of *mdt-15*(*tm2182*) mutants. a) The graph shows the average embryonic lethality of WT and *mdt-15*(*tm2182*) mutant worms grown on either *E. coli* OP50 or *C. aquatica* D1877 ($n = 3-5$). **** $P < 0.001$ for indicated comparisons, all other comparisons not significant, as assessed by two-way ANOVA with Tukey correction for multiple comparisons. b) The graph shows the average embryonic lethality of *mdt-15*(*tm2182*) mutant worms grown on either *E. coli* OP50 or *C. aquatica* D1877 for the P0 and F1 generations, as indicated ($n = 3$). **** $P < 0.001$ for indicated comparisons, all other comparisons not significant, as assessed by two-way ANOVA with Tukey correction for multiple comparisons. c) The graph shows the average embryonic lethality of WT and *mdt-15*(*tm2182*) mutant worms grown on either *E. coli* OP50, either unsupplemented or supplemented with methyl-cobalamin (Me-Cbl; $n = 5$). **** $P < 0.001$ for indicated comparisons, all other comparisons not significant, as assessed by two-way ANOVA with Tukey correction for multiple comparisons. d) The graph shows the average embryonic lethality of *mdt-15*(*tm2182*) mutant worms grown on either *E. coli* OP50, either unsupplemented or supplemented with Me-Cbl or adenosyl-cobalamin (Ado-Cbl) at the indicated concentrations ($n = 4$). **** $P < 0.001$ for indicated comparisons, all other comparisons not significant, as assessed by ordinary one-way ANOVA with Tukey correction for multiple comparisons. e) The graph shows the average embryonic lethality of WT (left) or *mdt-15*(*tm2182*) mutant (right) worms grown on *E. coli* OP50 on the indicated propionic acid concentrations and either unsupplemented or supplemented with methyl-cobalamin, as indicated ($n = 3-4$). * $P < 0.05$ and **** $P < 0.001$ for the indicated comparisons, as assessed by two-way ANOVA with Tukey correction for multiple comparisons.

when *C. elegans* has sufficient vitamin B12 ([MacNeil et al. 2013](#); [Watson et al. 2014](#)), require *mdt-15* for expression on *E. coli* OP50 ([Fig. 1b](#) and [Supplementary Fig. 1b and c](#)). We used RT-qPCR to quantify the expression of these genes in WT worms fed with *E. coli* OP50, WT worms fed with *C. aquatica* DA1877, and *mdt-15*(*tm2182*) mutants fed with *E. coli* OP50. This confirmed that *C. aquatica* DA1877 strongly downregulated the expression of *acdH-1*, *hphd-1*, *hach-1*, and *ech-6*, as expected ([MacNeil et al. 2013](#); [Watson et al. 2014](#)); in addition, we found that loss of

mdt-15 also downregulated *acdH-1*, *hphd-1*, *hach-1*, and *ech-6* ([Fig. 4a](#)). Thus, *mdt-15* is required to activate the expression of some shunt pathway genes in conditions of low vitamin B12 activity.

MDT-15 and NHR-10 coregulate propionic acid shunt breakdown genes

NHR-10 and NHR-68 regulate propionic acid shunt breakdown genes ([Bulcha et al. 2019](#)). We previously showed that NHR-68

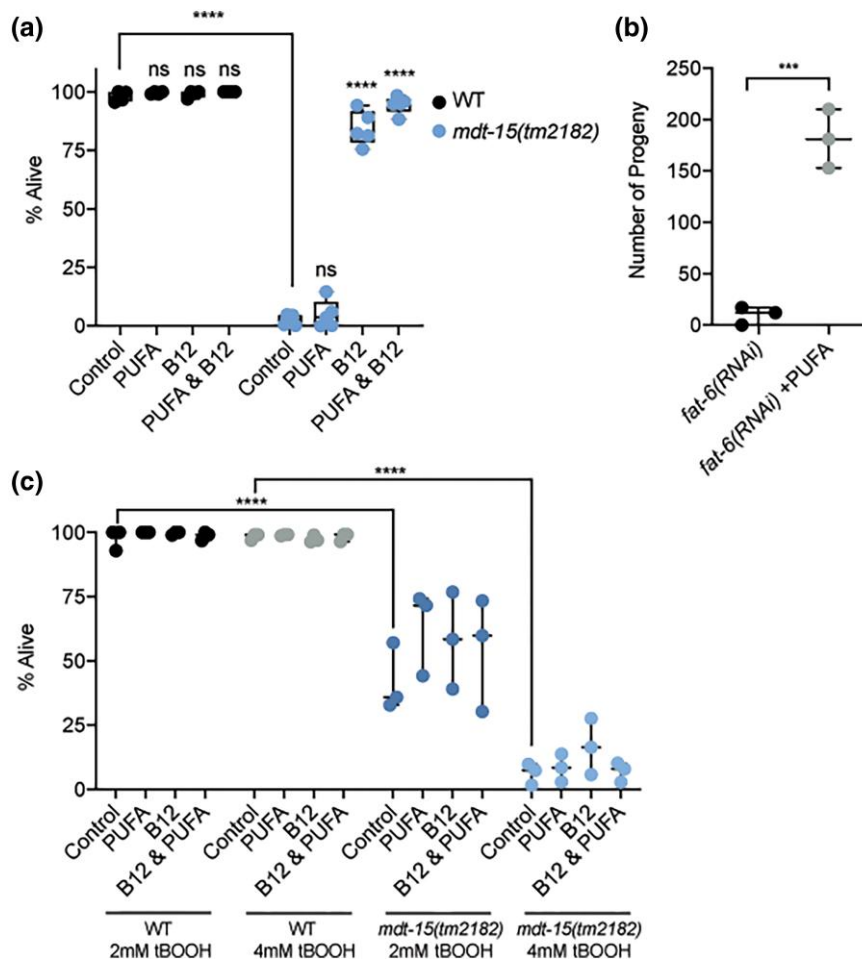


Fig. 3. PUFA diets do not rescue embryonic lethality and diets rich in vitamin B12 do not rescue the oxidative stress sensitivity of *mdt-15(tm2182)* mutants. a) The graph shows the average embryonic lethality of WT and *mdt-15(tm2182)* mutant worms grown on either *E. coli* OP50, either unsupplemented or supplemented with Me-Cbl, PUFAs, or Me-Cbl and PUFAs ($n = 4-5$). **** $P < 0.001$ for indicated comparisons, all other comparisons not significant, as assessed by two-way ANOVA with Tukey correction for multiple comparisons. b) The graph shows the number of progeny laid by *fat-6(RNAi)* worms with and without PUFA supplementation ($n = 3$). *** $P < 0.001$, unpaired Student's *t*-test. c) The graph shows the average number of WT and *mdt-15(tm2182)* mutant worms that are alive after growth on 2 mM or 4 mM tBOOH and supplemented with Me-Cbl, PUFAs, or Me-Cbl and PUFAs, as indicated ($n = 3$). **** $P < 0.001$ for indicated comparisons, ns = not significant, two-way ANOVA with Tukey correction for multiple comparisons.

does not bind MDT-15 in yeast two-hybrid (Y2H) assays (Taubert et al. 2006). In contrast, we and others detected NHR-10 binding to MDT-15 in Y2H screens (Arda et al. 2010; Reece-Hoyes et al. 2013). Quantification of binding using Y2H assays revealed that an NHR-10 bait protein indeed strongly binds to several MDT-15 prey proteins (Fig. 4b). Moreover, a construct containing only the KIX-domain of MDT-15 (aa 1-124), previously characterized as an NHR binding domain in MDT-15 (Taubert et al. 2006; Goh et al. 2014; Shomer et al. 2019), was sufficient to mediate this interaction (Fig. 4b). Overlap of gene sets dependent on NHR-10 and NHR-68 (Bulcha et al. 2019) and MDT-15 (this study) revealed that the genes controlled by each of these transcriptional regulators overlap substantially (Fig. 4c and Supplementary Table 8), with the shunt genes amongst the most strongly down-regulated genes in all of the mutants of these transcriptional regulators (Supplementary Fig. 1d and e). ORA of gene ontology terms revealed that the genes induced by all three transcriptional regulators as well as genes only coregulated by MDT-15 and NHR-10 are enriched for terms related to lipid and amino acid degradation, reflecting the presence of the shunt genes (Fig. 4d and e and Supplementary Table 9). ORA of the genes coregulated by

MDT-15 and NHR-68 revealed additional enrichment of gene sets related to detoxification (Fig. 4f and Supplementary Table 9). Overall, our data suggest that MDT-15 and NHR-10 likely interact physically and functionally to control the expression of propionic acid shunt breakdown and other genes *in vivo*, acting upstream of NHR-68.

Discussion

Vitamin B12 is an essential cofactor that is only synthesized by some species of bacteria. In contrast to the *E. coli* OP50 diet normally fed to *C. elegans* in the laboratory, a diet of *C. aquatica* DA1877 contains higher levels of vitamin B12, which influences a number of life history traits in worms, including brood size, developmental rate, and life span. Here, we show that vitamin B12 is essential for embryonic viability in *C. elegans* worms carrying a mutation in the *mdt-15* gene. Dissecting this requirement further, we find that *mdt-15* is required for the activation of genes in the propionic acid degradation shunt, which acts in parallel to the canonical vitamin B12-dependent propionic acid degradation pathway. Binding analysis with Y2H assays and comparison of

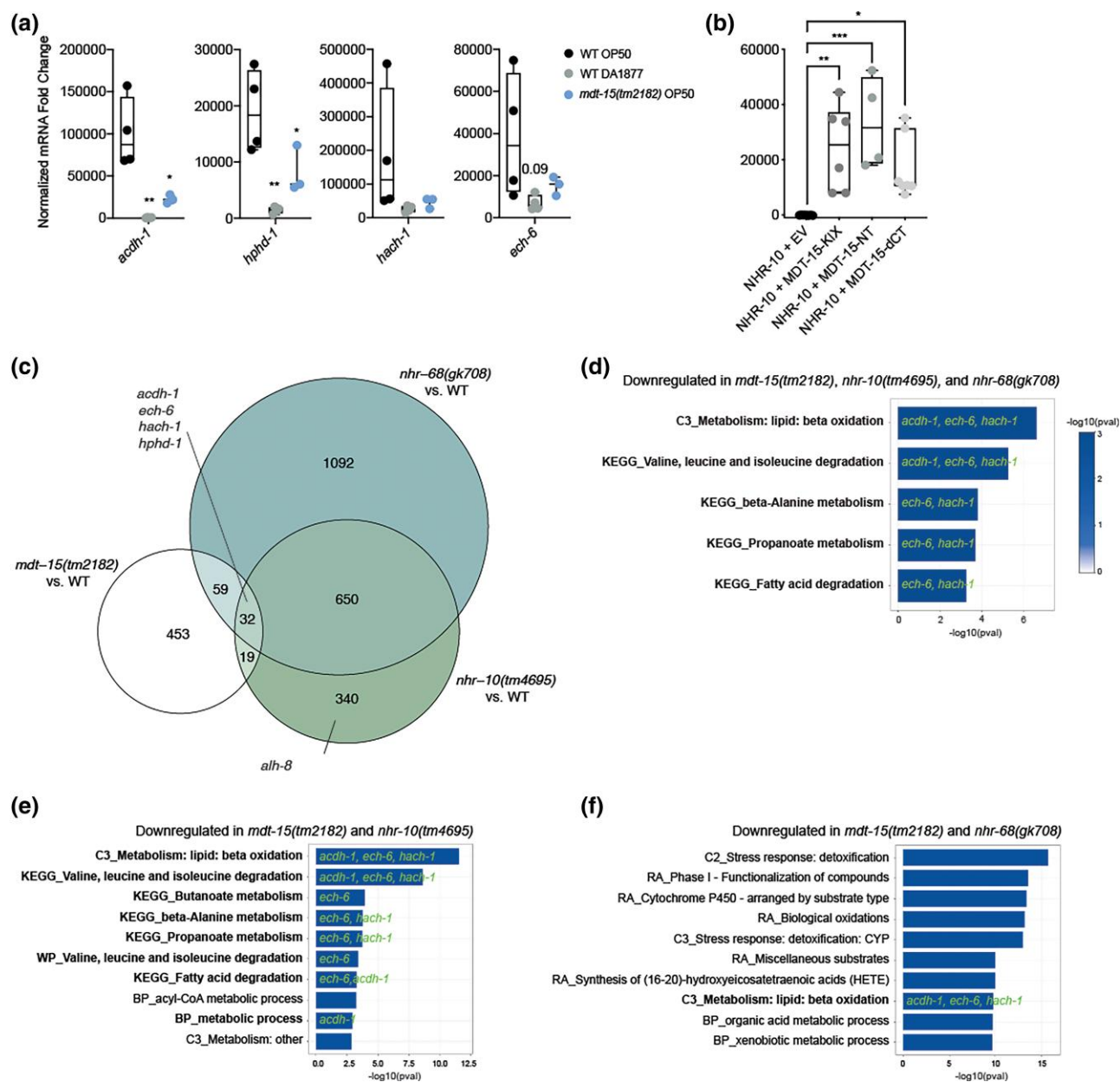


Fig. 4. MDT-15 regulates shunt gene expression and binds NHR-10 in Y2H assays. a) The graph indicates relative mRNA levels in L4 WT and *mdt-15(tm2182)* mutant worms grown on either *E. coli* OP50 or *C. aquatica* DA1877, as indicated ($n = 3-4$). * $P < 0.05$ and ** $P < 0.01$, ordinary one-way ANOVA with Tukey correction for multiple comparisons. b) Protein-protein interaction analysis using the Y2H system ($n = 4-7$). The graph shows the average interaction strength (arbitrary units, AU) between an NHR-10 prey and the following baits: empty vector (EV; negative control), MDT-15-KIX (aa 1-124), MDT-15-NT (aa 1-338), or MDT-15 Δ CT (aa 1-598). Statistical analysis: * $P < 0.05$, ** $P < 0.01$, and *** $P < 0.005$ vs NHR-10 + EV, ordinary one-way ANOVA, multiple comparisons, Dunnett correction. c) The Venn diagram shows the overlap of genes downregulated in *mdt-15(tm2182)*, *nhr-10(tm4695)*, and *nhr-68(gk708)* mutants (Adj.P or $P < 0.05$ and $\log_{2}FC < 0$) compared to WT. Both the overlap between *mdt-15(tm2182)* and *nhr-10(tm4695)* mutants (51 genes, hypergeometric $P = 0.00048$; platform size = 18,605) and the overlap between *mdt-15(tm2182)* and *nhr-68(gk708)* mutants (91 genes, hypergeometric $P = 1.41e^{-06}$; platform size = 18,605) are statistically significant. The location of shunt genes (*acdh-1*, *ech-6*, *hach-1*, *hphd-1*, and *alh-8*) is annotated. Full lists of genes in each dataset are shown in [Supplementary Tables 2 and 6-7](#). Lists of genes present in the overlaps are shown in [Supplementary Table 8](#). d-f) The bar plots show top the 10 (or fewer, if less than 10 were statistically significant) overrepresented gene sets ($P < 0.005$, Adj.P < 0.25) in the following overlaps: d) triple overlap of *mdt-15(tm2182)*, *nhr-10(tm4695)*, and *nhr-68(gk708)* (5 gene sets total); e) overlap of *mdt-15(tm2182)* and *nhr-10(tm4695)* (11 gene sets total); and f) overlap of *mdt-15(tm2182)* and *nhr-68(gk708)* (42 gene sets total). Width and color of the bars represent $-\log_{10}(\text{pval})$. Gene sets containing one or more shunt genes are highlighted in bold, with the relevant shunt genes listed. The following databases were selected for ORA analysis: Kyoto Encyclopedia of Genes and Genomes (KEGG), Reactome Pathway (RA), WikiPathways (WP), WormCat Category 2 (C2), WormCat Category 3 (C3), and Gene Ontology: Biological Processes (BP). pval, P-value; padj, adjusted P-value. Full lists of overrepresented gene sets are shown in [Supplementary Table 9](#).

mutant transcriptomes suggest that MDT-15 may interact with NHR-10 to regulate shunt gene expression, thus adapting *C. elegans* metabolism in conditions where propionic acid degradation through the canonical vitamin B12-dependent mechanisms is not possible.

The strong embryonic lethality phenotype of the *mdt-15(tm2182)* mutant and its virtually complete rescue by diets rich in vitamin B12 is interesting. Many of the phenotypes of this mutant (larval arrest, fecundity, life span, and mobility) are largely rescued by supplementation of worms with unsaturated fatty

acids, yet, these have no effect on the embryonic lethality phenotype. In line with the phenotype we observed, RNAi and/or mutation of *acdH-1*, *hach-1*, *hphd-1*, and *alh-8* also causes embryonic arrest, which for *acdH-1*, *hphd-1*, and *alh-8* manifests specifically when vitamin B12 is low in abundance (Gönczy et al. 2000; Simmer et al. 2003; Sönnichsen et al. 2005; Watson et al. 2016); similarly, *ech-6* RNAi caused larval arrest, albeit not embryonic arrest (possibly due to RNAi efficiency variability). The loss of shunt gene function therefore phenocopies loss of *mdt-15* with regard to embryonic viability. It is not fully clear why vitamin B12, and by inference propionic acid detoxification, is crucial during embryonic development. Possibly, the rapid growth associated with embryonic development leads to transient increases in propionic acid breakdown intermediates, perhaps because specific amino acids or fatty acids are in demand.

Mutation of *nhr-10* or *nhr-68* causes larval arrest/delay when propionic acid is present in the media (Bulcha et al. 2019), phenocopying the propionic acid sensitivity of larval development seen after mutation/depletion of *mdt-15* or the shunt genes. Curiously, however, *nhr-10* or *nhr-68* mutation or depletion was not found to cause embryonic or larval arrest (Gönczy et al. 2000; Kamath et al. 2003; Simmer et al. 2003; MacNeil et al. 2013; Bulcha et al. 2019). Bulcha et al. (2019) observed that *acdH-1* expression in *nhr-10* and *nhr-68* mutants is reduced, but not completely abrogated; possibly, *mdt-15* mutation lowers the expression of *acdH-1* (and other shunt genes) below the levels required for embryonic development. This could be because MDT-15 acts as a coregulator for one (or more) of the 44 other transcription factors that regulate *acdH-1* (and perhaps, other shunt genes) (Macneil et al. 2015). These include NHR-114 and SBP-1, which bind MDT-15 (Yang et al. 2006; Arda et al. 2010) and impinge on shunt gene activity (Giese et al. 2020; Qin et al. 2022). Further work will be required to delineate the details of this regulation.

We did not test whether the other vitamin B12 activated pathway, methionine synthesis, is affected by *mdt-15* mutation. We reasoned that even if methionine synthesis was low, these worms should receive an adequate methionine supply from their *E. coli* diet. However, methionine synthesis is linked to the one-carbon cycle, in particular, the metabolism of folate to its biologically active form, tetrahydrofolate. Interestingly, *mdt-15* mutants express lower levels of the folate transporter *folT-2*, as determined by microarray and RT-qPCR analysis (Taubert et al. 2008). However, no overt phenotypes have been reported for *folT-2* depletion by RNAi (Gönczy et al. 2000; Simmer et al. 2003; Sönnichsen et al. 2005), perhaps because *folT-1* and *folT-3* compensate for *folT-2* loss.

Our study adds to the growing list of specific gene regulatory programs that are implemented by partnerships between MDT-15 and NHRs (and other TFs). For example, we and others showed that NHR-49 and MDT-15 interact physically and regulate the expression of numerous fatty acid metabolism genes, which in turn affects numerous phenotypes of *mdt-15* mutants, including viability, life span, fecundity, mobility, and others (Taubert et al. 2006; Yang et al. 2006). Recent studies suggest that NHR-49 and MDT-15 also interact to promote resistance to several stresses, including starvation, oxidative stress, hypoxia, and pathogen resistance (Goh et al. 2018; Hu et al. 2018; Dasgupta et al. 2020; Hummell et al. 2021; Wani et al. 2021; Doering et al. 2022). MDT-15 also binds NHR-86 (Reece-Hoyes et al. 2013), and both factors regulate the expression of innate immune response genes and ensure survival in response to infection with the pathogen *Pseudomonas aeruginosa*, with NHR-86 directly sensing the presence of pathogen-derived toxic metabolite (Peterson et al. 2019, 2023). Furthermore, an interaction between MDT-15 and HIZR-1 (aka NHR-33) promotes the expression of

heavy metal response genes through the high-zinc activated regulatory element (Roh et al. 2015; Shomer et al. 2019). The data presented here suggest that NHR-10 and MDT-15 interact to transcriptionally induce propionic acid degradation shunt genes when propionic acid levels are high, and/or vitamin B12 levels are low. Interestingly, HIZR-1 directly binds the essential metal zinc as well as nonessential, toxic cadmium (Warnhoff et al. 2017; Earley et al. 2021), and HIZR-1 binding to MDT-15 is strongly increased in the presence of such ligands (Shomer et al. 2019). Possibly, metabolites linked to the propionic acid degradation pathway could similarly be ligands for NHR-10 (Bulcha et al. 2019), although its very short chain length distinguishes it from other such molecules that serve as NHR ligands. It is also possible that upstream metabolites, such as branched-chain amino acids and longer odd-chain fatty acids, act as ligands for NHR-10. Alternatively, the MDT-15–NHR-10 interaction may be altered by posttranslational modifications, or due to NHR-10 dimerizing with a different partner, e.g. forming an NHR-10 dimer that interacts more strongly with MDT-15.

In summary, we report a novel interaction between the gene encoding the transcriptional regulator *mdt-15* and vitamin B12, an essential micronutrient. We hypothesize that when vitamin B12 levels are low, and/or propionic acid levels are high, NHR-10 and MDT-15 interaction is stimulated, which in turn allows increased expression of the shunt genes and permits normal embryonic development despite low vitamin B12 availability. It will be interesting to determine whether this mechanistic role for MDT-15 and HNF4-like nuclear receptors is conserved in mammals, especially in view of shunt gene activation by exogenous propionic acid in cultured liver cancer cell lines (Watson et al. 2016).

Data availability

The data underlying this article are available in the article, in its online [Supplementary material](#), and at Gene Expression Omnibus online (GSE220955). All reagents are available upon request.

[Supplementary material](#) is available at G3 online.

Acknowledgements

We thank the Taubert Lab members and Amy K. Walker (UMass Medical School, Worcester, MA, USA) for comments on the manuscript.

Funding

Some strains were provided by the CGC, which is funded by the NIH Office of Research Infrastructure Programs (P40 OD010440). Grant support was from the Canadian Institutes of Health Research (CIHR; PJT-153199 to ST), the Natural Sciences and Engineering Research Council of Canada (NSERC; RGPIN-2018-05133 to ST), and a BCCHR Healthy Starts Catalyst grant. GYSG and JY were supported by BCCHR and UBC scholarships, KD by a NSERC CGS-D and UBC scholarships, AB by an NSERC-USRA studentship, and ST by a Canada Research Chair.

Conflicts of interest statement

The author(s) declare no conflict of interest.

Literature cited

- Arda HE, Taubert S, Macneil LT, Conine CC, Tsuda B, Van Gilst M, Sequerra R, Doucette-Stamm L, Yamamoto KR, Walhout AJ. Functional modularity of nuclear hormone receptors in a *Caenorhabditis elegans* metabolic gene regulatory network. *Mol Syst Biol*. 2010;6(1):367. doi:10.1038/msb.2010.23.
- Bito T, Watanabe F. Biochemistry, function, and deficiency of vitamin B12 in *Caenorhabditis elegans*. *Exp Biol Med*. 2016;241(15):1663–1668. doi:10.1177/1535370216662713.
- Bolger AM, Lohse M, Usadel B. Trimmomatic: a flexible trimmer for Illumina sequence data. *Bioinformatics*. 2014;30(15):2114–2120. doi:10.1093/bioinformatics/btu170.
- Boukouris AE, Zervopoulos SD, Michelakis ED. Metabolic enzymes moonlighting in the nucleus: metabolic regulation of gene transcription. *Trends Biochem Sci*. 2016;41(8):712–730. doi:10.1016/j.tibs.2016.05.013.
- Brenner S. The genetics of *Caenorhabditis elegans*. *Genetics*. 1974;77(1):71–94. doi:10.1093/genetics/77.1.71.
- Bulcha JT, Giese GE, Ali MZ, Lee Y-U, Walker MD, Holdorf AD, Yilmaz LS, Brewster RC, Walhout AJM. A persistence detector for metabolic network rewiring in an animal. *Cell Rep*. 2019;26(2):460–468.e4. doi:10.1016/j.celrep.2018.12.064.
- Cheng X, Yan J, Liu Y, Wang J, Taubert S. eVITTA: a web-based visualization and inference toolbox for transcriptome analysis. *Nucleic Acids Res*. 2021;49(W1):W207–W215. doi:10.1093/nar/gkab366.
- Dasgupta M, Shashikanth M, Gupta A, Sandhu A, De A, Javed S, Singh V. NHR-49 transcription factor regulates immunometabolic response and survival of *Caenorhabditis elegans* during *Enterococcus faecalis* infection. *Infect Immun*. 2020;88(8):e00130–20. doi:10.1128/IAI.00130-20.
- Deodato F, S. Boenzi, F. M. Santorelli, C. Dionisi-Vici, 2017 Methylmalonic and propionic aciduria. *Am J Medical Genetics Part C Seminars Medical Genetics* 142C(2):104–112. doi:10.1002/ajmg.c.30090.
- Doering KR, Cheng X, Milburn L, Ratnappan R, Ghazi A, Miller DL, Taubert S. Nuclear hormone receptor NHR-49 acts in parallel with HIF-1 to promote hypoxia adaptation in *Caenorhabditis elegans*. *Elife*. 2022;11:e67911. doi:10.7554/eLife.67911.
- Earley BJ, Cubillas C, Warnhoff K, Ahmad R, Alcantar A, Lyon MD, Schneider DL, Kornfeld K. Cadmium hijacks the high zinc response by binding and activating the HIZR-1 nuclear receptor. *Proc National Acad Sci*. 2021;118(42):e2022649118. doi:10.1073/pnas.2022649118.
- Froese DS, Fowler B, Baumgartner MR. Vitamin B12, folate, and the methionine remethylation cycle—biochemistry, pathways, and regulation. *J Inherit Metab Dis*. 2019;42(4):673–685. doi:10.1002/jimd.12009.
- Giese GE, Walker MD, Ponomarova O, Zhang H, Li X, Minevich G, Walhout AJM. *Caenorhabditis elegans* methionine/S-adenosylmethionine cycle activity is sensed and adjusted by a nuclear hormone receptor. *Elife*. 2020;9:e60259. doi:10.7554/eLife.60259.
- Goh GYS, Martelli KL, Parhar KS, Kwong AWL, Wong MA, Mah A, Hou NS, Taubert S. The conserved Mediator subunit MDT-15 is required for oxidative stress responses in *Caenorhabditis elegans*. *Aging cell*. 2014;13(1):70–79. doi:10.1111/accel.12154.
- Goh GYS, Winter JJ, Bhansali F, Doering KRS, Lai R, Lee K, Veal EA, Taubert S. NHR-49/HNF4 integrates regulation of fatty acid metabolism with a protective transcriptional response to oxidative stress and fasting. *Aging Cell*. 2018;17(3):e12743. doi:10.1111/accel.12743.
- Gönczy P, Echeverri C, Oegema K, Coulson A, Jones SJM, Copley RR, Dupéron J, Oegema J, Brehm M, Cassin E, et al. Functional genomic analysis of cell division in *C. elegans* using RNAi of genes on chromosome III. *Nature*. 2000;408(6810):331–336. doi:10.1038/35042526.
- Grants JM, Goh GYS, Taubert S. The Mediator complex of *Caenorhabditis elegans*: insights into the developmental and physiological roles of a conserved transcriptional coregulator. *Nucleic Acids Res*. 2015;43(4):2442–2453. doi:10.1093/nar/gkv037.
- Grants JM, Ying LTL, Yoda A, You CC, Okano H, Sawa H, Taubert S. The Mediator kinase module restrains epidermal growth factor receptor signaling and represses vulval cell fate specification in *Caenorhabditis elegans*. *Genetics*. 2016;202(2):583–599. doi:10.1534/genetics.115.180265.
- Hartman JH, Widmayer SJ, Bergemann CM, King DE, Morton KS, Romersi RF, Jameson LE, Leung MCK, Andersen EC, Taubert S, et al. Xenobiotic metabolism and transport in *Caenorhabditis elegans*. *J Toxicol Environ Health B Crit Rev*. 2021;24(2):51–94. doi:10.1080/10937404.2021.1884921.
- Hou NS, Gutschmidt A, Choi DY, Pather K, Shi X, Watts JL, Hoppe T, Taubert S. Activation of the endoplasmic reticulum unfolded protein response by lipid disequilibrium without disturbed proteostasis in vivo. *Proc Natl Acad Sci USA*. 2014;111(22):E2271–80. doi:10.1073/pnas.1318262111.
- Hu Q, D'Amora DR, Macneil LT, Walhout AJM, Kubiseski TJ. The *Caenorhabditis elegans* oxidative stress response requires the NHR-49 transcription factor. *G3 (Bethesda)*. 2018;8(12):3857–3863. doi:10.1534/g3.118.200727.
- Hummell NA, Revtovich AV, Kirienko NV. Novel immune modulators enhance *Caenorhabditis elegans* resistance to multiple pathogens. *MSphere*. 2021;6(1):e00950–20. doi:10.1128/mSphere.00950-20.
- Husted AS, Trauelsen M, Rudenko O, Hjorth SA, Schwartz TW. GPCR-mediated signaling of metabolites. *Cell Metab*. 2017;25(4):777–796. doi:10.1016/j.cmet.2017.03.008.
- Kamath RS, Fraser AG, Dong Y, Poulin G, Durbin R, Gotta M, Kanapin A, Le Bot N, Moreno S, Sohrmann M, et al. Systematic functional analysis of the *Caenorhabditis elegans* genome using RNAi. *Nature*. 2003;421(6920):231–237. doi:10.1038/nature01278.
- Larsson J, Gustafsson P. A case study in fitting area-proportional Euler diagrams with ellipses using eulerr. *Proceedings of International Workshop on set visualization and reasoning*. 2018;2116:84–91. <https://cran.r-project.org/package=euler>
- Lee D, An SWA, Jung Y, Yamaoka Y, Ryu Y, Goh GYS, Beigi A, Yang J-S, Jung GY, Ma DK, et al. MDT-15/MED15 permits longevity at low temperature via enhancing lipidostasis and proteostasis. *PLoS Biol*. 2019;17(8):e3000415. doi:10.1371/journal.pbio.3000415.
- Lee D, Jeong D-E, Son HG, Yamaoka Y, Kim H, Seo K, Khan AA, Roh T-Y, Moon DW, Lee Y, et al. SREBP and MDT-15 protect *C. elegans* from glucose-induced accelerated aging by preventing accumulation of saturated fat. *Genes Dev*. 2015;29(23):2490–2503. doi:10.1101/gad.266304.115.
- Macneil LT, Pons C, Arda HE, Giese GE, Myers CL, Walhout AJM. Transcription factor activity mapping of a tissue-specific in vivo gene regulatory network. *Cell Syst*. 2015;1(2):152–162. doi:10.1016/j.cels.2015.08.003.
- MacNeil LT, Watson E, Arda HE, Zhu LJ, Walhout AJM. Diet-induced developmental acceleration independent of TOR and insulin in *C. elegans*. *Cell*. 2013;153(1):240–252. doi:10.1016/j.cell.2013.02.049.
- Patro R, Duggal G, Love MI, Irizarry RA, Kingsford C. Salmon provides fast and bias-aware quantification of transcript expression. *Nat Methods*. 2017;14(4):417–419. doi:10.1038/nmeth.4197.
- Peterson ND, Cheesman HK, Liu P, Anderson SM, Foster KJ, Chhaya R, Perrat P, Thekkiniaht J, Yang Q, Haynes CM, et al. The nuclear hormone receptor NHR-86 controls anti-pathogen responses in *C. elegans*. *Plos Genet*. 2019;15(1):e1007935. doi:10.1371/journal.pgen.1007935.

- Peterson ND, Tse SY, Huang QJ, Wani KA, Schiffer CA, Pukkila-Worley R. Non-canonical pattern recognition of a pathogen-derived metabolite by a nuclear hormone receptor identifies virulent bacteria in *C. elegans*. *Immunity*. 2023;56(4):768–782.e9. doi:10.1016/j.immuni.2023.01.027.
- Pukkila-Worley R, Feinbaum RL, McEwan DL, Conery AL, Ausubel FM. The evolutionarily conserved Mediator subunit MDT-15/MED15 links protective innate immune responses and xenobiotic detoxification. *Plos Pathog*. 2014;10(5):e1004143. doi:10.1371/journal.ppat.1004143.
- Qin S, Wang Y, Li L, Liu J, Xiao C, Duan D, Hao W, Qin C, Chen J, Yao L, et al. Early-life vitamin B12 orchestrates lipid peroxidation to ensure reproductive success via SBP-1/SREBP1 in *Caenorhabditis elegans*. *Cell Rep*. 2022;40(12):111381. doi:10.1016/j.celrep.2022.111381.
- Reece-Hoyes JS, Pons C, Diallo A, Mori A, Shrestha S, Kadreppa S, Nelson J, DiPrima S, Dricot A, Lajoie BR, et al. Extensive rewiring and complex evolutionary dynamics in a *C. elegans* multiparameter transcription factor network. *Mol Cell*. 2013;51(1):116–127. doi:10.1016/j.molcel.2013.05.018.
- Ritchie ME, Phipson B, Wu D, Hu Y, Law CW, Shi W, Smyth GK. Limma powers differential expression analyses for RNA-sequencing and microarray studies. *Nucleic Acids Res*. 2015;43(7):e47. doi:10.1093/nar/gkv007.
- Robinson MD, McCarthy DJ, Smyth GK. Edger: a bioconductor package for differential expression analysis of digital gene expression data. *Bioinformatics*. 2010;26(1):139–140. doi:10.1093/bioinformatics/btp616.
- Roh HC, Dimitrov I, Deshmukh K, Zhao G, Warnhoff K, Cabrera D, Tsai W, Kornfeld K. A modular system of DNA enhancer elements mediates tissue-specific activation of transcription by high dietary zinc in *C. elegans*. *Nucleic Acids Res*. 2015;43(2):803–816. doi:10.1093/nar/gku1360.
- Schneider-Poetsch T, Yoshida M. Along the central dogma—controlling gene expression with small molecules. *Annu Rev Biochem*. 2018;87(1):391–420. doi:10.1146/annurev-biochem-060614-033923.
- Shomer N, Kadhim AZ, Grants JM, Cheng X, Alhusari D, Bhanshali F, Poon AFY, Lee MY, Muhuri A, Park JI, et al. Mediator subunit MDT-15/MED15 and nuclear receptor HIZR-1/HNF4 cooperate to regulate toxic metal stress responses in *Caenorhabditis elegans*. *PLoS Genet*. 2019;15(12):e1008508. doi:10.1371/journal.pgen.1008508.
- Simmer F, Moorman C, van der Linden AM, Kuijk E, van den Berghe PVE, Kamath RS, Fraser AG, Ahringer J, Plasterk RHA. Genome-wide RNAi of *C. elegans* using the hypersensitive rrf-3 strain reveals novel gene functions. *Plos Biol*. 2003;1(1):e12. doi:10.1371/journal.pbio.0000012.
- Soneson C, Love MI, Robinson MD. Differential analyses for RNA-seq: transcript-level estimates improve gene-level inferences. *F1000Res*. 2016;4:1521. doi:10.12688/f1000research.7563.2.
- Sönnichsen B, Koski LB, Walsh A, Marschall P, Neumann B, Brehm M, Alleaume A-M, Artelt J, Bettencourt P, Cassin E, et al. Full-genome RNAi profiling of early embryogenesis in *Caenorhabditis elegans*. *Nature*. 2005;434(7032):462–469. doi:10.1038/nature03353.
- Steimel A, Suh J, Hussainkhel A, Deheshi S, Grants JM, Zapf R, Moerman DG, Taubert S, Hutter H. The *C. elegans* CDK8 Mediator module regulates axon guidance decisions in the ventral nerve cord and during dorsal axon navigation. *Dev Biol*. 2013;377(2):385–398. doi:10.1016/j.ydbio.2013.02.009.
- Suganuma T, Workman JL. Chromatin and metabolism. *Annu Rev Biochem*. 2018;87(1):27–49. doi:10.1146/annurev-biochem-062917-012634.
- Taubert S, Gilst MRV, Hansen M, Yamamoto KR. A Mediator subunit, MDT-15, integrates regulation of fatty acid metabolism by NHR-49-dependent and -independent pathways in *C. elegans*. *Gene Dev*. 2006;20(9):1137–1149. doi:10.1101/gad.1395406.
- Taubert S, Hansen M, Gilst MRV, Cooper SB, Yamamoto KR. The Mediator subunit MDT-15 confers metabolic adaptation to ingested material. *PLoS Genet*. 2008;4(2):e1000021. doi:10.1371/journal.pgen.1000021.
- Vozdek R, Long Y, Ma DK. The receptor tyrosine kinase HIR-1 coordinates HIF-independent responses to hypoxia and extracellular matrix injury. *Sci Signal*. 2018;11(550):eaat0138. doi:10.1126/scisignal.aat0138.
- Wani KA, Goswamy D, Taubert S, Ratnappan R, Ghazi A, Irazoqui JE. NHR-49/PPAR- α and HLH-30/TFEB cooperate for *C. elegans* host defense via a flavin-containing monooxygenase. *eLife*. 2021;10:e62775. doi:10.7554/eLife.62775.
- Warnhoff K, Roh HC, Kocsisova Z, Tan C-H, Morrison A, Crosswell D, Schneider DL, Kornfeld K. The nuclear receptor HIZR-1 uses zinc as a ligand to mediate homeostasis in response to high zinc. *PLoS Biol*. 2017;15(1):e2000094. doi:10.1371/journal.pbio.2000094.
- Watson E, Macneil LT, Arda HE, Zhu LJ, Walhout AJM. Integration of metabolic and gene regulatory networks modulates the *C. elegans* dietary response. *Cell*. 2013;153(1):253–266. doi:10.1016/j.cell.2013.02.050.
- Watson E, Macneil LT, Ritter AD, Yilmaz LS, Rosebrock AP, Caudy AA, Walhout AJM. Interspecies systems biology uncovers metabolites affecting *C. elegans* gene expression and life history traits. *Cell*. 2014;156(4):759–770. doi:10.1016/j.cell.2014.01.047.
- Watson E, Olin-Sandoval V, Hoy MJ, Li C-H, Louise T, Yao V, Mori A, Holdorf AD, Troyanskaya OG, Ralser M, et al. Metabolic network rewiring of propionate flux compensates vitamin B12 deficiency in *C. elegans*. *eLife*. 2016;5:e17670. doi:10.7554/eLife.17670.
- Yang F, Vought BW, Satterlee JS, Walker AK, Sun Z-YJ, Watts JL, DeBeaumont R, Mako Saito R, Hyberts SG, Yang S, et al. An ARC/Mediator subunit required for SREBP control of cholesterol and lipid homeostasis. *Nature*. 2006;442(7103):700–704. doi:10.1038/nature04942.